2002

Bearing System In Dynamic Loading Including Solid Contact And Wear

H. J. Wisbeck
EMBRACO

A. L. Manke
EMBRACO

A. T. Prata
Federal University of Santa Catarina

BEARING SYSTEM IN DYNAMIC LOADING INCLUDING SOLID CONTACT AND WEAR

Hilbert J. Wisbeck, Research Engineer, Embraco –Empresa Brasileira de Compressores S.A.
R. Rui Barbosa, 1020 – 89219-901 Joinville, SC Brazil
Tel.:+55 (47) 441-2749; Fax: +55 (47) 441-2225
E-Mail: Wilbert_J_Wisbeck@embraco.com.br

*__Adilson L. Manke__, Research Engineer, Embraco –Empresa Brasileira de Compressores S.A.
R. Rui Barbosa, 1020 – 89219-901 Joinville, SC Brazil
Tel.:+55 (47) 441-2715; Fax: +55 (47) 441-2225
E-Mail: Adilson_L_Manke@embraco.com.br

Alvaro T. Prata, Professor, UFSC – Universidade Federal de Santa Catarina,
Dpto. Eng. Mecânica, Campus Universitário, 88040-900 Florianópolis, SC Brazil
Tel.: +55(48) 234-5691; Fax: +55 (48) 234-1519
E-Mail: prata@nrva.ufsc.br

ABSTRACT

In small reciprocating compressors for household applications the compressor shaft is placed vertically and supports a dynamic load associated to the transversal piston movement. Usually, for design purposes, the bearings are treated separately which precludes a precise description of the shaft orbit. In the present investigation both the main and the secondary journal bearings are modeled coupled and simultaneously, allowing for shaft misalignment within the bearings. A new computational methodology is introduced and tested to determine the pressure distribution in both bearings via a direct procedure. Solid contact and wearing are both allowed to occur causing a significant impact on the frictional power and a minor effect on the shaft orbit.

INTRODUCTION

Classical references in the literature related to bearing under dynamic loading are Campbell *et al.* (1967), that presented an extended review of early works on this subject, with theoretical and experimental results, and Jones (1982) that introduced a methodology for dynamic loading including oil holes and grooves as well as starvation effects. Most available works explore formulations and results for just one bearing, with the shaft perfectly aligned with the bearing axis. Effects of shaft misalignment on bearings operating under static loading were investigated by Pinkus and Bupara (1979), and Vijayaraghavan *et al.* (1990).

The present work deals with two bearings working coupled under a dynamic loading, for a small reciprocating hermetic compressor employed for household applications. The formulation includes shaft misalignment during the load cycle. Solid contact is allowed to occur and is modeled using the classic Coulomb law, where the friction force is related to the normal force through a friction coefficient. Recently, Zhou and Rogers (1997) used this same classic relation in a work on the effects of the squeeze film and the solid contact between a tube and its holder in a heat exchanger. Similarly, Sun and Jing Xu (1995) employed Coulomb law in the analysis of a bearing starting characteristics considering the solid friction, without including lubrication.

Despite of the high effort to fully understand the radial bearings behavior under every circumstances, only in recent works wear effects have been considered. Del Din and Kassfeldt (1999) presented friction and wear results for radial bearings. Their experiments investigated the influence of oil type, oil contamination, temperature, and shaft rotation on the friction values and bearings wear index. Regarding modeling, a literature survey indicated no previous work related to contact and wear prediction for radial bearing operating under dynamic loading, and in this regard the present paper aims to contribute towards a comprehensive approach for bearing system simulation.

CASE STUDY DESCRIPTION

To explore the problem geometry to be considered here figure 1 was prepared. According to the figure, the shaft stands vertically with the main bearing (1st bearing) on the top and the secondary bearing (2nd bearing) on the bottom. This geometry reproduces the situation encountered in small hermetic compressors where the electric motor is placed on the lower part of the shaft and drives the piston on its upper end. The piston moves horizontally in a reciprocating motion imposing an alternating load on the shaft. In turn, the shaft describes a periodic misalign trajectory within the bearings.

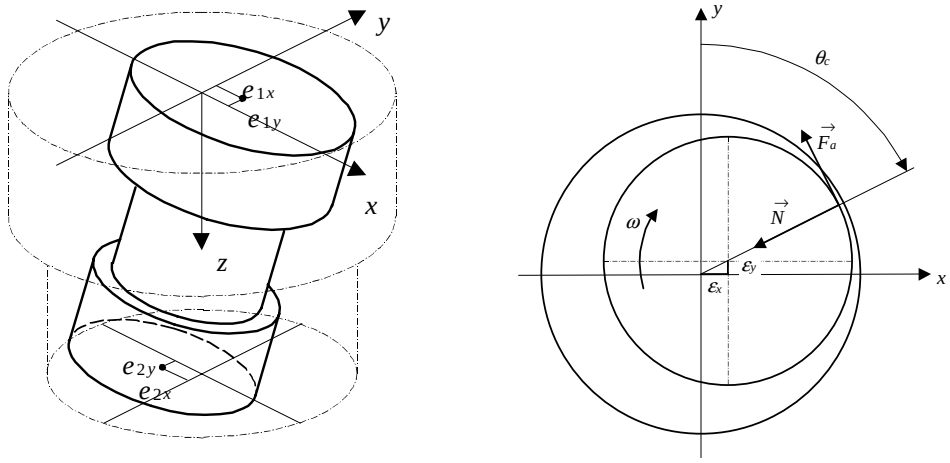

(a) bearing system (b) contact forces

Figure 1: Problem Geometry.

The shaft trajectory is governed by the forces and moments acting on it, and is defined at each time step by the eccentricities e_{1x}, e_{1y}, e_{2x} and e_{2y} according to figure 1a. Neglecting the shaft inertia, balances of forces, F, and moments, M, along *x* and *y* directions require that

$$\sum F_x = F_{h_x} + \sum_i W_{i_x} = 0 \qquad \sum F_y = F_{h_y} + \sum_i W_{i_y} = 0 \tag{1}$$

$$\sum M_x^0 = M_{h_x}^0 + \sum_i W_{i_y} z_i = 0 \qquad \sum M_y^0 = M_{h_y}^0 + \sum_i W_{i_x} z_i = 0 \tag{2}$$

where the index *h* represents the hydrodynamic action, and the indexes *x* and *y* represent the components in the x and y directions, respectively; *W* is the external load, and *z* is the axial position where the load is applied. The hydrodynamic forces and moments, F_h and M_h, respectively, are obtained integrating the pressure field determined from the Reynolds equation. The external load imposed on the shaft is known, as a function of the compression process and the inertia forces of the moving components.

In the present work, the main objective is to obtain the shaft misalign trajectory defined by the extreme eccentricities, and to that extent use will be made of equations (1) and (2). The pressure field along the oil film required in calculating the hydrodynamic forces and moments depends on the oil film thickness that is associated to the local eccentricities. In presence of shaft misalignment and wear, the local oil film thickness, *h*, can be written as

$$h = c\left(1 - \varepsilon_x \operatorname{sen}\theta - \varepsilon_y \cos\theta\right) + dh_e + dh_m \tag{3}$$

where $\varepsilon = e/c$, and c is the radial clearance between bearing and shaft; dh_e and dh_m depend on the bearing position and define the wear depth in that point on the shaft and on the journal bearing, respectively. Considering that the midline of the shaft is straight, it is possible to write *h* as a linear function of the extreme eccentricities e_{1x}, e_{1y}, e_{2x} and e_{2y}.

Employing the expressions for h and its derivatives, the Reynolds equation for the journal bearings under consideration can be written as

$$\frac{\partial}{\partial\theta}\left(f(\varepsilon)\frac{\partial p}{\partial\theta}\right)+\frac{\partial}{\partial\xi}\left(f(\varepsilon)\frac{\partial p}{\partial\xi}\right)+F\dot{\varepsilon}_{1_x}+G\dot{\varepsilon}_{2_x}+H\dot{\varepsilon}_{1_y}+I\dot{\varepsilon}_{2_y}=g(\varepsilon) \tag{4}$$

where $\dot{\varepsilon}$ is the time derivative of the eccentricities and F, G, H, I, $f(\varepsilon)$ and $g(\varepsilon)$ are known functions.

The Reynolds equation together with the balances of forces and moments suffice to determine the shaft trajectory. In presence of metallic contact between the parts, equations (1) and (2) need to be corrected to include the contact force. The contact force is the sum of the normal and friction forces according to

$$F_{c_x}=F_{a_x}+N_x \qquad\qquad F_{c_y}=F_{a_y}+N_y \tag{5}$$

where F_c is the contact force, F_a is the friction force, and N is the normal force acting on the surfaces.

Referring to Fig. 1b, it is possible to write the contact force as

$$F_{c_x}=-F_a\cos\theta_c-N\,\mathrm{sen}\,\theta_c \qquad\qquad F_{c_y}=+F_a\,\mathrm{sen}\,\theta_c-N\cos\theta_c \tag{6}$$

where θ_c is the contact angular position. Employing Coulomb law, that is, $F_a=\mu_f N$, where μ_f is the friction coefficient, equation (6) results in

$$F_{c_x}=(-\mu_f\cos\theta_c-\mathrm{sen}\,\theta_c)N \qquad\qquad F_{c_y}=(+\mu_f\,\mathrm{sen}\,\theta_c-\cos\theta_c)N \tag{7}$$

During the contact, the normal force is unknown and to closure the problem an additional equation is required. The equation to be used prescribes a fixed value for the oil film thickness, such as $h(\theta_c,z_c)=f(R_q)$, where z_c is the contact axial position and R_q is the surfaces roughness. Here, it will be considered that $f(R_q)$ is a non-null constant independent of the applied load. Prescription of a fixed oil film thickness during contact represents a simplified version of a more elaborate model where the normal contact force is related to the real contact area which, in turn, depend on the elastic and plastic deformations of the surface roughness (Rabinowicz, 1995).

For computational purposes it is convenient to relate the restriction equation for the oil film thickness, $h(\theta_c,z_c)=f(R_q)$, with the velocities of the bearings extremes (time derivative of the extreme eccentricities). To that extent, first the local oil film thickness, h, is written as a linear function of the extreme eccentricities; next, a first order approximation is employed for the variation of the extreme eccentricities with time as

$$\varepsilon^{\tau+\Delta\tau}=\varepsilon^{\tau}+\dot{\varepsilon}^{\tau+\Delta\tau}\Delta\tau \tag{8}$$

where $\Delta\tau$ is the increment on the crankshaft angle. From that, it is possible to rewrite the restriction equation, $h(\theta_c,z_c)=f(R_q)$, as a function of the velocities on the bearing extremes, $\dot{\varepsilon}$, as

$$A\dot{\varepsilon}_{1_x}+B\dot{\varepsilon}_{2_x}+C\dot{\varepsilon}_{1_y}+D\dot{\varepsilon}_{2_y}=E \tag{9}$$

in which A, B, C, D e E are known coefficients at each time step. In presence of solid contact, equation (9) is the required additional equation needed to calculate the contact normal force, N.

Attention will now be turned to the determination of the worn volume. The worn volume, V_d, due to the direct contact between the shaft and the journal bearings is calculated using the Archard law as presented by Rabinowicz (1995),

$$V_d = kNR\Delta\tau / H_{em} \tag{10}$$

where H_{em} is the hardness of the parts material, and k is a wear constant. In the present formulation the worn volume is equally divided between shaft and journal bearing, considering that shaft and journal bearing surfaces have the same properties. When contact is detected and the normal force is determined, V_d can be calculated. The worn geometry is obtained interposing shaft and bearing so that the intercepted volume equals that calculated by Archard law, according to

$$\int (\Delta dh) dA = V_d \tag{11}$$

where Δdh is the depth that must be removed on the contact point vicinities, considering that half is taken from the shaft and half from the bearing.

METHODOLOGY

Integration of the Reynolds equation was performed using a finite volume methodology (Patankar, 1980, and Ferziger and Peric, 1996). To this extent the computational domain is divided in small non-overlapping cartesian control volumes, and for each control volume an algebraic equation is obtained for the pressure at that control volume. A typical equation relating pressure at the control volume with the neighboring pressures and the four extreme shaft velocities can be written as,

$$-A_P p_P + \sum A_{nb} p_{NB} + F\dot{\varepsilon}_{1_x} + G\dot{\varepsilon}_{2_x} + H\dot{\varepsilon}_{1_y} + I\dot{\varepsilon}_{2_y} = g(\varepsilon) \tag{12}$$

where A_P e A_{nb} are the finite volume method coefficients.

For n control volumes on the computational grid, equation (12) represents a set of n algebraic equations. Those equations together with the force and moment equations form a linear system with n+4 equations, where the unknowns are the n pressures and the four extreme shaft velocities.

In presence of solid contact it is necessary to include the contact forces on the balance equations for force and moment. Because of the presence of the unknown normal force, the restriction condition for the oil film thickness, equation (9), has to be added to the linear system. For solid contact on both bearings at the same time, two normal forces on the equilibrium equations and two oil film thickness restriction equations are required.

To verify contact occurrence, at each time step the oil film thickness is compared to the value assigned by $f(R_q)$. If one or more thickness values is less than $f(R_q)$, contact is assumed to occur at the point of the smallest oil film thickness. Next, θ_c and $\xi_c = z/R$ are determined and the contact forces and the oil film thickness restriction equation are both included on the linear system. On the other hand, to verify the instant of the contact interruption, it is necessary to look for the normal force value: if it is negative, the hydrodynamic effects are able to sustain the load and contact no long occurs. At that instant, the restriction equation for the oil film thickness and the contact force should be removed from the linear system.

The linear system was solved by Gaussian elimination. The Gauss algorithm was optimized, since the system is sparse and its structure is well defined. In this regard, some rules were applied to ensure that the elimination occurred only where it was necessary.

Cavitation was treated using the Reynolds condition for the cavitation boundary. The linear system was solved throughout the entire clearance between bearings and shaft. When the value of a calculated pressure was found to be less than the cavitation pressure, pressure was set equal to the cavitation pressure for its neighboring equations. This procedure assured that the null pressure and the null pressure gradient boundary condition were respected at the cavitation region.

Because the balances of forces and moments were computed simultaneously with the pressure field, very few iterations at each time interval were require for a converged solution. In fact iterations were only required because the coefficients of the algebraic equations depend on the eccentricities and these non-linearities were updated at each iteration. The procedure just described was performed at each time step until convergence was achieved. The shaft orbit can then be obtained including the occurrence of solid contact.

In addition to the computational mesh needed for integration of the Reynolds equation, another mesh was employed to precisely determine the worn region. To that extent, during contact the shaft is interposed against the bearing until the interposed depth integrated along the worn region yielded the worn volume obtained from Archard law. It should be noted that the integrated volume depends on the interposition between shaft and bearing and can be related to the shaft eccentricity. The interposition volume was obtained increasing the eccentricity until the worn volume was achieved; use was made of the bisection method to determine the eccentricity required to mach the worn volume.

RESULTS AND DISCUSSION

To validate the formulation and the computational code, several tests were performed including some comparisons with available results found in the literature. In the paper of Campbell *et al*. (1967) experimental and numerical results were presented for the connecting rod big end of a Ruston and Hornsby 6 VEB-X Mk III Diesel engine. The bearing load and dimensions were included in the referenced paper. Figure 2 shows a comparison of the journal trajectory calculated by the present work and experimental and theoretical results presented by Campbell. As can be seen from the figure, a very good agreement prevailed among all the journal orbits.

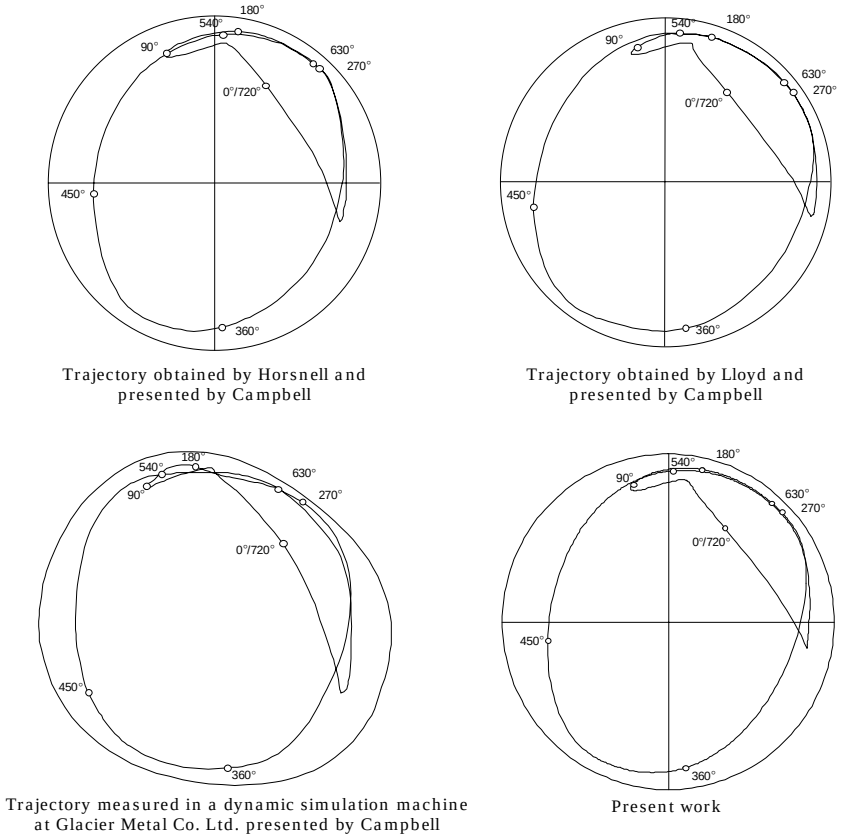

Figure 2: Results for big-end connecting rod bearing of Ruston and Hornsby Diesel engine

To present some results where the solid contact occurs, use was made of a bearing system and a load cycle of a small reciprocating hermetic compressor. The computations were performed for three values for the solid friction coefficient, 0 (zero), 0.1 and 0.4. The input data used in the simulations are presented in the Table 1.

Table 1. Entry data for the reciprocating compressor employed in the simulations.

- Rotation, N *(clockwise)*	3520 rev/min	- Gap between bearings, g	32.3 mm
- Angular velocity, ω	368.6 rad/s	- Radial clearance, c	10.0 μm
- Bearings radius, R	9.5 mm	- Solid contact factor, $f(R_a)$	$0.02c = 0.2\mu$m
- 1st bearing width, W_1	14.0 mm	- Viscosity, μ	2.28 mPa·s
- 2nd bearing width, W_2	7.5 mm	- Solid friction coefficients, μ_f	0, 0.1, 0.4

Values of mean friction power losses are presented in the Table 2 for different values of the solid friction coefficients. Although the presented formulation allows for solid contact also in the 2nd bearing, it did not occur for the cases investigated here. The power losses values were divided by the maximum power loss value obtained for the 1st bearing with a solid friction coefficient equal to zero. As observed in the table, the power loss is directly affected by the solid friction coefficient, showing the importance of using a good estimate for this coefficient to predict the total power loss in the bearing system.

Table 2. Cycle-averaged friction power losses on the bearings.

Solid Friction Coefficient ⇨	0.0	0.1	0.4
1st bearing	0.746	3.085	7.476
2nd bearing	0.384	0.384	0.384
Bearing system	1.130	3.469	7.860

Despite the high range of friction coefficient considered, the lateral oil leakage from both bearings was practically unchanged due to the small trajectory distortion.

Because of the presence of solid contact, wear is expected to occur. Results for wear will now be explored for a friction coefficient of 0.1. In what follows, the hardness of the shaft and bearings surfaces, H_{em}, was taken equal to 300 kg/mm^2, and the wear constant, k, was made equal to 10^{-7}. To avoid the long computational times required to simulate the material removal from the shaft and bearing surfaces during wear, a special procedure was adopted. First some initial cycles were performed without including wear until the periodic trajectory is established. Next, the wear routine was switched on and off in alternating cycles. During the cycle in which the wear routine was activated, material is removed changing the geometry, and, in turn, the shaft trajectory. For the next cycle the wear routine was deactivated allowing for the stability and convergence of the trajectory.

Another important aspect during the simulation of wear refers to the extrapolation of the worn volume. In a real process the worn volume during a single cycle is extremely small and thousands of cycles are required to obtain a significant change in geometry due to wear. To avoid performing the simulation during such a large number of cycles, which would be prohibitive, the worn volume determined during a single cycle was multiplied by a large factor extrapolating the results for several cycles. In this regard it was admitted a linear behavior of wear with time.

Results for the time evolution of the volume of worn material with time (from shaft and 1st bearing) are presented in figure 3. The initial cycles required to stabilize the shaft trajectory are not shown in the figure and the dots correspond to the cycles were the wear routine was activated. As previously discussed, the extrapolation factor employed in preparing figure 4 was 4000. It is interesting to note that as time proceeds the amount of removed material is reduced indicating an accommodation of the geometry towards eliminating the solid contact.

Figure 4 presents the bearing trajectory (represented by the extreme eccentricities on the external boundaries of the bearings) without considering wear (dashed line), and in presence of wearing and after geometry stabilization (solid line). In the case without considering wear, contact occurred for the 1st bearing, and at the

contact region the shaft rolled to the right side over the bearing surface, due to the instantaneous high friction, as expected, considering that the shaft is rotating clockwise. The external circumference indicated in the figure corresponds to the original bearing geometry, before material is removed. The instantaneous friction power loss corresponding to the two trajectories of figure 4 are shown in figure 5. As expected, at the location where solid contact occurs, there is an intense peak on the friction power loss. For this value of friction factor the peak is of two orders of magnitude above the power loss without solid contact. After geometry accommodation due to wear, the peak disappears and for the entire cycle the instantaneous friction power loss assume the same order of magnitude.

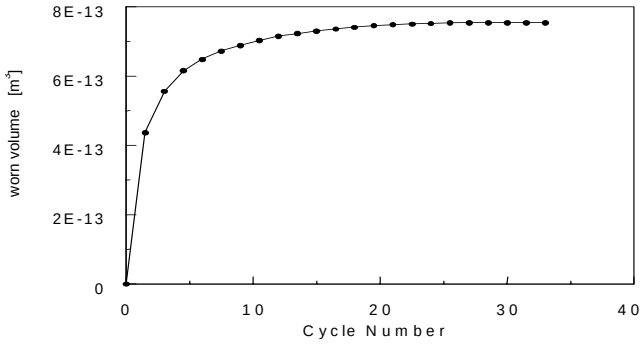

Figure 3: Evolution of the volume of worn material

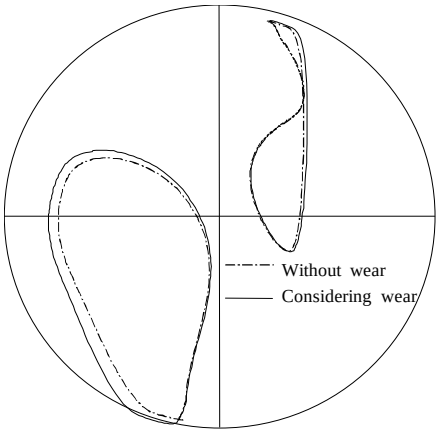

Figure 4: Effect of wear on the shaft trajectory

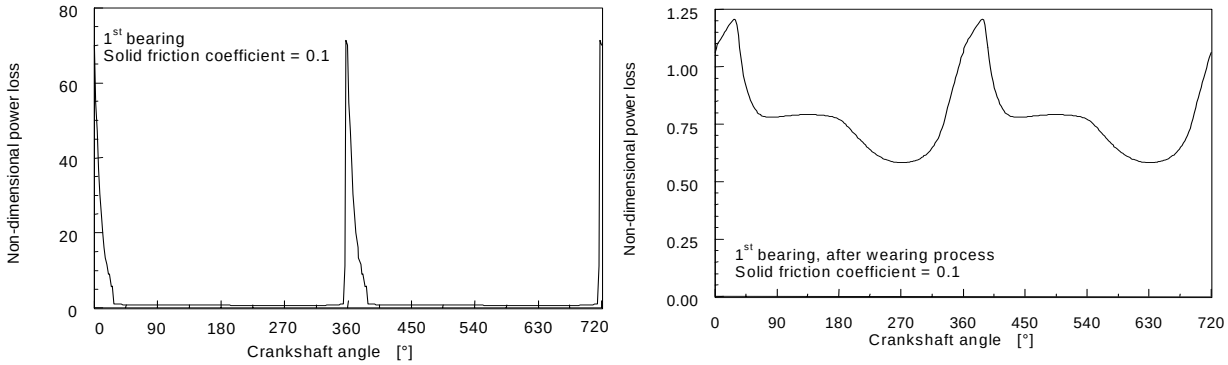

(a) before the wearing process (b) after the wearing process

Figure 5: Effect of wear on the instantaneous friction power loss on the 1st bearing

CONCLUSIONS

In this work a direct dynamic model for the lubrication process of bearing systems including solid friction and wear has been presented. The solution of this kind of problem using a direct algorithm seems to be the more convenient way to deal with the coupling between the Reynolds equation and the equations for the shaft dynamics. Furthermore, the formulation and methodology adopted allowed for the inclusion of solid contact and wear. Among other observations, it was shown that the shaft trajectory was just slightly influenced by large variations in the solid friction coefficient, suggesting that stability problems because of the solid contact against the bearing is unlikely to occur. The lateral oil leakage from both bearings is virtually insensible to changes on the solid friction coefficient, explained by the low distortion of the shaft trajectory with this coefficient. The solid friction coefficient has a great influence on the friction power loss. Results for the instantaneous friction power loss in presence of solid contact and with friction coefficient of 0.1 showed peak values of two orders of magnitude greater than those encountered in non-contact situations.

Also, in all simulations with solid contact, as time proceeded it was observed the asymptotic reduction of the wear process as result of the geometry accommodation, with eventual elimination of the solid contact.

ACKNOWLEDGEMENTS

This study was presented at the 56th STLE Annual Meeting in May of 2001. Due to public diversity, it was opted to presenting it, with some alterations, also in this 2002 International Compressor Engineering Conference at Purdue.

REFERENCES

Campbell, J., Love, P. P., Martin, F. A., Rafique, S. O., 1967, Bearings for Reciprocating Machinery: A Review of the Present State of Theoretical, Experimental and Service Knowledge, Proc. Inst. of Mech. Engrs., vol. 182 Pt 3A, pp. 51-74.

Del Din, M., Kassfeldt, E., 1999, Wear Characteristics with Mixed Lubrication Conditions in a Full Scale Journal Bearing, Wear 232, pp. 192-198.

Jones, G. J., Crankshaft Bearing: Oil Film History, 1982, Proceedings 9th Leeds-Lyon Symposium of Tribology, pp.83-88.

Ferzinger, J. H. and Peric, M., 1996, Computational Methods for Fluid Dynamics, Springer Verlag.

Patankar, S. V., 1980, Numerical Heat Transfer and Fluid Flow, Hemisphere Publishing Corp., New York.

Pinkus, O., Bupara S. S., 1979, Analysis of Misaligned Grooved Journal Bearings, Transactions ASME, Journal of Lubrication Technology, vol. 101, pp. 503-509.

Rabinowicz, E., 1995, Friction and Wear of Materials, 2.ed, John Wiley & Sons Inc., New York.

Sun, D. C., Jing Xu, 1995, A Study of the Starting Characteristics of an Unlubricated Journal Bearing, Transactions ASME, Journal of Tribology, vol. 117, pp. 216-223.

Vijayaraghavan, D., Keith Jr., T. G., 1990, Analysis of a Finite Grooved Misaligned Journal Bearing Considering Cavitation and Starvation Effects, Transactions ASME, Journal of Tribology, vol. 112, pp. 60-67.

Zhou, T., Rogers, R. J., 1997, Simulation of Two-Dimensional Squeeze Film and Solid Contact Forces Acting on a Heat Exchanger Tube, Journal of Sound and Vibration, vol. 203(4), pp. 621-639.